Design of new kind of tunable micro ring resonator

Ying YuHai[1,2]

(1. College of Electronics Information Engineering, Anhui University, Hefei 230039, China;
2. Department of Information Engineering, Anhui Broadcasting Movie and Television Vocational College, Hefei 230011, China)

Abstract: In order to improve mems-sensor application and the characteristic of parameters, the micro-nano optical fiber ring resonator structure was designed, which was a small size, low dissipation, and high quality factor. The characteristics of micro-nano optical fiber and optical transmission mode were analyzed theoretically, through the electric field of transfer matrix, the function relationships among wavelength, perimeter, effective refractive index for micro ring resonator were obtained under the acceleration effect. The results of simulation analysis show that electric field of waveguide fluctuates significantly, and coupling efficiency of waveguide is better. Spectral intensity and 3 dB bandwidth change smaller. Q value reaches 104. When mass increases 10 g, output spectrum drifts to the right about 3 nm. Acceleration and drift quantity of resonant wavelength are almost linear. Drift of resonant wavelength can be used to measure acceleration. The results can provide variety of optical waveguide devices for all-optical networks and micro-electromechanical system.

Key words: optical microring; refractivity; cavity; acceleration

CLC number: O203 **Document code:** A **DOI:** 10.3788/IRLA201645.0620002

新型的可调谐微环谐振器的设计

应毓海[1,2]

(1. 安徽大学 电子信息工程学院,安徽 合肥 230039;
2. 安徽广播影视职业技术学院 信息工程系,安徽 合肥 230011)

摘 要: 为了改进微机电系统中的传感器应用范围和特性参数,采用微纳光纤制作了环形谐振腔结构,设计的结构具有尺寸小、损耗低,品质因素高等优点。理论上分析了微纳光纤的光传输模式特性,通过电场的传数矩阵推导了谐振腔中的速度变化与光强变化间的关系, 得到了加速度作用下微环谐振腔的谐振波长、周长、有效折射率的变化值间的函数关系。仿真结果分析表明:设计的微环波导电场波动明显,耦合效率较好;光谱强度和 3 dB 带宽变化较小,Q 值达到 10^4;在质量块每增加 10 g 时,输出光谱图约向右漂移 3 nm;加速度与谐振波长漂移量基本呈线性关系,可以通过谐振波长的漂移量来实现对加速度的测量。研究结果能够为全光网络和微机电系统提供实现多种功能的光波导器件。

关键词: 微纳光纤; 折射率; 谐振腔; 加速度

收稿日期:2015-10-05; **修订日期:**2015-11-03

基金项目:国家 863 计划课题(2013AA122202);安徽省教育厅重点科研项目(KJ2014A033)

作者简介:应毓海(1965-),男,副教授,硕士,主要从事电子通信技术方面的研究。Email:yyh1737@sina.com

0 Introduction

The emergence of ruby laser and laser in the early 1960s set the development of the field of optical communication. Later, with the continuous development of the laser technology, optics permeated and fused with other disciplines and created many new branched or edged disciplines[1-2]. With the development of optical fiber communication technology, the performance of optical communication networks must be improved and operating costs must be reduced, especially because the core technology has enabled the miniaturization and integration of optical waveguide devices [3-5]. At the same time, all future optical networks must have new optical waveguide devices that can perform many functions. An optical microring resonator possesses some great qualities, such as high Q value and low modal volume [6-7]. The resonator has a small and compact structure, is low cost, exhibits low loss, and has a good wavelength selection; thus, it has been extensively researched and applied in optical communication networks [8]. In 2010, Smith introduced the concepts of Bloch dielectric constant and Bloch permeability and analyzed coupling between differential medium electric resonance and magnetic resonance[9-10]. In 2013, Payam Rabiei from the Institute of Optics and Photonics and Saeed Khan et al. from the Department of Electrical and Computer Engineering of the University of Florida adopted a method called selective oxidation of refractory metals to synthesize a microring resonator and optical waveguide using submicron Ta_2O_5 on a silicon substrate.This novel method eliminates the rough surface problem of a side wall, which is caused by the dry etching method in making a waveguide[11-12]. At present, manufacturing photonic devices is geared toward integration and miniaturization. A micro-nano optical fiber, which is the main topic in this research, is a type of optical waveguide structure of mesoscopic scale. Compared with an ordinary fiber, a micro-nano optical fiber displays a large relative refractive value and a strong binding capacity to light[13]. In addition, a ring resonator composed of micro-nano optical fibers has a small size, low loss, and high quality factor; these features can help improve the sensitivity of a sensor fabricated with a micro-nano optical fiber ring[14-15]. In this research, an acceleration sensor is designed based on literature and the resonator theory of micro-nano optical fibers.

1 Transmission theory analysis

1.1 Light transmission using micro-nano optical fibers

The optical waveguide length of microlight devices is generally very short. Hence, we must first regard the lighted transmission as lossless in this micro-nano optical so that Maxwell′s equation, which reflects the light transmitted in the micro-nano optical fiber, can be simplified into a wave equation. In this research, the electric and magnetic fields are changed with time and space as

$$\nabla^2 E=\mu\varepsilon\frac{\partial^2 E}{\partial t^2} \tag{1}$$

and

$$\nabla^2 H=\mu\varepsilon\frac{\partial^2 H}{\partial t^2} \tag{2}$$

where E is the electric field intensity, H is the magnetic field intensity, μ is medium permeability, and ε is the dielectric constant. We suppose that the refractive index of the micro-nano optical fiber is unchanged in the axial direction. If the method of normal optical waveguide is adopted to analyze the micro-nano optical fiber, then the optical field of the transmitted light in the micro-nano optical fiber can be represented by

$$\begin{bmatrix} E \\ H \end{bmatrix}(x,y,z,t)=\begin{bmatrix} e \\ h \end{bmatrix}(x,y)\mathrm{e}^{i(\omega t-\beta z)} \tag{3}$$

If the mode field satisfies the wave equation, then

$$(\nabla^2+n^2k^2-\beta^2)e=0 \tag{4}$$

and

$$(\nabla^2+n^2k^2-\beta^2)h=0 \tag{5}$$

Furthermore, a numerical analysis can derive the

numerical solution for the propagation constant β. The micro-nano optical fibers, which use air for cladding or silica as a core layer, are respectively inputted to an incident light of 700 nm wavelength. The relationship between the propagation constant β and the micro-nano optical fiber diameter D is shown in Figure 1.

As shown in Figure 1, when the micro-nano optical fiber diameter is reduced to a particular value, only an HE_{11} model that exhibits a single-mode transmitted mechanism (black solid line in figure) exists in the micro-nano optical fiber. Other higher-order models appear when the micro-nano optical fiber diameter is larger than a particular value.

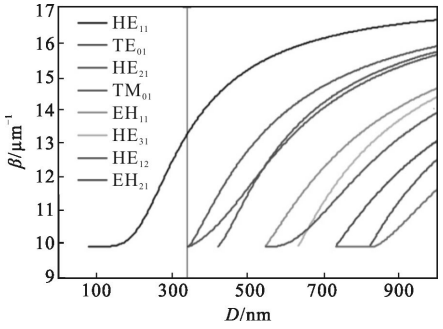

Fig.1 Propagation constant when the wavelength is 700 nm

1.2 Resonant cavity transmission and accelerated sensor

Every light field in the resonant cavity can be described by the following form, which is a number matrix:

$$\begin{bmatrix} E_o \\ E_{r1} \end{bmatrix} = \begin{bmatrix} t_r & i\kappa_r \\ i\kappa_r & t_r \end{bmatrix} \mathrm{e}^{j\beta_r L_{\mathrm{eff}}} \begin{bmatrix} E_i \\ E_{r2} \end{bmatrix} \tag{6}$$

where E_i and E_o represent the optical field intensity of the input and output ports of the single straight waveguide, respectively; E_{r1} and E_{r2} are the light field intensity of the cavity side in the field of coupled; L_{eff} is the effective coupling length of resonant cavity in the coupling area; and t_r and κ_r are the amplitude attenuation factor and the coupling coefficient, respectively. Moreover,

$$E_{r2} = \tau_r \exp(i\beta_r L_t) E_{r1} \tag{7}$$

where $\tau_r = \exp(-\alpha_r L_r)$ represents the amplitude attenuation factor, which is related to the attenuation coefficient α_r and length when light is transmitted in the cavity; refers to the perimeter of the cavity; $L_r = 2\pi R + 2L_S$ is the propagation constant of the cavity; $\beta_r = 2\pi n_{\mathrm{eff}}/\lambda$ and $\beta_r L_t$ represents the changes of the phase when light is transmitted in the cavity. When the external acceleration affects the mass block, the fixed structure obviously causes deformation because of stress. Stress can be expressed as:

$$\sigma(x) = \frac{3maL_1}{bh^2}\left(\frac{2x}{L_1} - 1\right) \tag{8}$$

where m is the quality of the mass block, a is the acceleration, L_1 is the distance from the mass block to the fixed end, b is the width of the fixed end, and h is the thickness of the fixed end. Let a single straight micro-nano optical fiber and a microring resonator be the sensing elements when light is inputted from the imported end and transmitted through a straight waveguide. According to coupled-mode theory, coupling occurs in the straight waveguide and cavity. Moreover, the light that occurs during the coupling enters the cavity and causes resonance in the resonant cavity. The resonant wavelength drift distance in the output port and the outputted intensity changes of the same wavelength are tested to detect acceleration. The concrete working principle to perform the acceleration test is as follows: Sensing mass block occurs when acceleration is applied to the mass block in the fixed end, thereby causing displacement along a sensitive direction. In this way, the fixed end causes deformation because of the effect of stress. At this point, the perimeter of the resonator, which is a sensitive element, changes with fixed end deformation. When the fixed end is stressed and deformation occurs because of the elastic-optic effect, the effective refractive index of the micro-nano optical fiber resonator, which is solidified on the surface of the fixed end, can also cause change. We can obtain the value acceleration by testing the deformation of micro-nano optical cavity and focusing on the fixed end, the changes of stress, and the resonance wavelength drift distance in the micro-nano optical fiber cavity. The

drift variation depends on the variation of the microring effective refractive index and microring perimeter, of which a specific relationship can be expressed as follows:

$$\frac{\Delta\lambda}{\lambda}=\frac{\Delta L}{L}+\frac{\Delta n}{n} \tag{9}$$

where $\Delta\lambda$,ΔL and Δn represent the changed values of the microring resonator resonance wavelength, perimeter, and effective refractive index after the acceleration effect, respectively.

2 Analysis of simulation results

2.1 Microring optical transmission

Detailed and accurate parameters of the linear and circular waveguides are as follows: Linear waveguide (0, −4) (10, −4) and radius of circular waveguide(8,0.5): 1.8.

The parameter settings of the linear and circular waveguides are 0.5 for the width and 1 for the height. The pattern and refractive index of incident plane are shown in Figure 2.

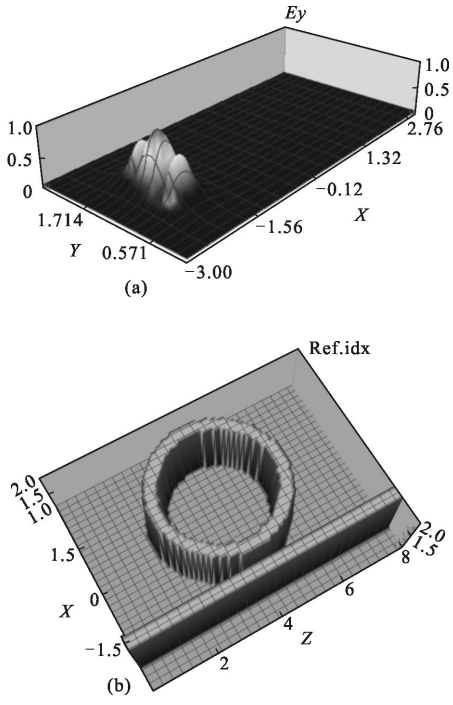

Fig.2 Input light plane, the refractive index distribution

The results of microring resonator *Ey* (DFT) is shown in Figure 3. The result of changing the two optical waveguide distance is shown in Figure 4. As shown in Figures 3 and 4, the designed microring waveguide *Ey* significantly fluctuates, and its coupling efficiency is good.

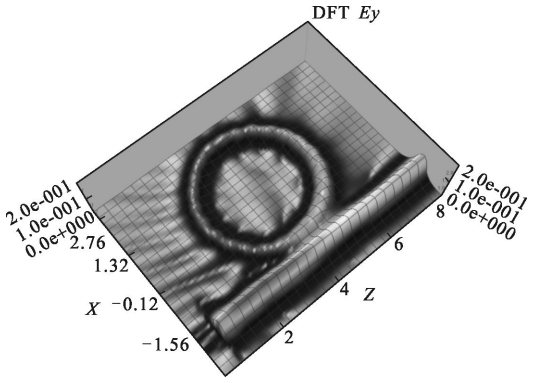

Fig.3 *Ey* (DFT)

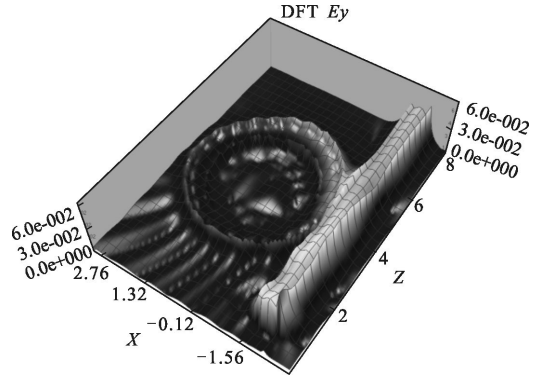

Fig.4 Change after two optical waveguide spacing *Ey* (DFT)

2.2 Analysis of the acceleration sensor results

According to the theoretical analysis, we can use a method that detects the resonant wavelength drift distance in the output port to calculate the acceleration. The method can achieve a high-sensitivity and wide-range detection. Figure 5 shows the sensor output spectra, of which the acceleration value ranges from 0 to 50 and increases by 10 g/t.

As shown in the graph, the spectral intensity and 3 dB bandwidth in the output spectra did not change. The Q value can reach only when the resonant wavelength moves to the right, which clearly shows that the resonance wavelength drifts in the output spectrum during increasing acceleration. When the

acceleration increases by 10 g/t, the output spectrum drifts to the right by approximately 3 nm. Thus, we can measure the acceleration on the basis of the resonant wavelength drift. The curve in Figure 6 shows the relationship between the resonant wavelength and acceleration,

As shown in Figure 6, the relationship between the acceleration and the resonant wavelength drift is linear by fitting the relation between the 0 –50 g/t acceleration and the resonant wavelength drift. The above results can be used as a theoretical reference for applying a waveguide structure.

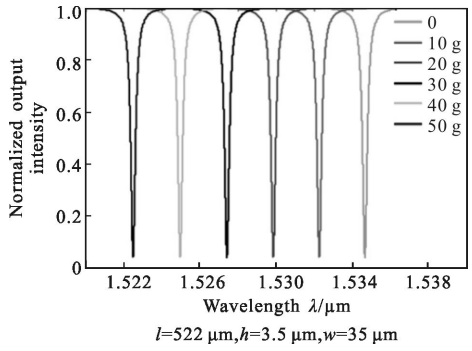

Fig.5 Under different acceleration output spectra

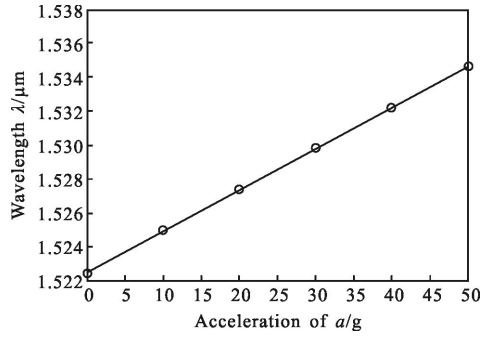

Fig.6 Resonant wavelengths and acceleration diagram

3 Conclusion

Micro-nano optical fibers feature small size, low bending loss, evanescent field intensity, and simple manufacturing process that are different from traditional single mode fibers or integrated optical waveguides. In this paper, we propose a microacceleration sensor on the basis of the characteristics of the micro-nano optical fiber. We analyzed the micro-nano optical fibers, the transmitted theory of the ring resonator, and other related features. The wavelength drift detection method was adopted to perform the acceleration test. The results of this study contribute theoretically and practically to the development of microelectromechanical systems.

References:

[1] Yang L G, Jyu S S, Chow C W, et al. A 110 GHz passive mode-locked fiber laser based on a nonlinear silicon-micro-ring-resonator[J]. ***Laser Physics Letters***, 2014, 11(6): 065101.

[2] Li H, Dong B, Zhang Z, et al. A transparent broadband ultrasonic detector based on an optical micro-ring resonator for photoacoustic microscopy[J]. ***Scientific Reports***, 2014, 4(3): 4496–4496.

[3] Hu S, Qin K, Kravchenko I I, et al. Suspended micro-ring resonator for enhanced biomolecule detection sensitivity[C]// Proceedings of SPIE, 2014, 8933(1): 893306–893306–7.

[4] Chun–Ta W, Yuan–Cheng L, Jui–Hao Y, et al. Electrically tunable high Q–factor micro-ring resonator based on blue phase liquid crystal cladding [J]. ***Optics Express***, 2014, 22 (15): 17776–17781.

[5] Ryota W, Mikio F, Ken-Ichiro Y, et al. Time-bin entangled photon pair generation from Si micro-ring resonator [J]. ***Optics Express***, 2015, 23(2): 1103–1113.

[6] Mohammadzadeh M H, Rostami A, Dolatyari M, et al. Optical bistability in a single-bus InGaAs micro-ring resonator array [J]. ***Optik-International Journal for Light and Electron Optics***, 2014, 125(14): 3573–3577.

[7] Yan S, Li M, Luo L, et al. Optimisation design of coupling region based on SOI micro-ring resonator [J]. ***Micromachines***, 2014, 6(1): 151–159.

[8] Akhlaghi M. Optimization of wide-band Si-$Si_{1-x}Ge_x$ micro ring resonator Raman amplifier using particle swarm optimization method[J]. ***Journal of Modern Optics***, 2014, 62 (5): 336–339.

[9] Zhang Z, Dong B, Li H, et al. Theoretical and experimental studies of distance dependent response of micro-ring resonator-based ultrasonic detectors for photoacoustic microscopy [J]. ***Journal of Applied Physics***, 2014, 116(14): 144501–144501.

[10] Matsumoto A, Matsushita A, Takei Y, et al. Intermixing of InP-based quantum dots and application to micro-ring resonator wavelength-selective filter for photonic integrated

devices[J]. ***Appl Phys Express***, 2014, 7(9): 5880-5885.

[11] Rostami A, Mohammadzadeh M H, Dolatyari M, et al. An all-optical switch/photodetection at 1 550 nm, based on a micro-ring resonator array [J]. ***Optik-International Journal for Light and Electron Optics***, 2014, 125(16): 4529-4533.

[12] Mohammadzadeh M H, Rostami A, Rostami G, et al. Transient and steady state analysis of micro ring resonator array based photodetector in optical communication wavelength (linear and nonlinear operation) [J]. ***Optik-International Journal for Light and Electron Optics***, 2014, 125(15): 3935-3942.

[13] Berglund M, Persson A, Thornell G. Operation characteristics and optical emission distribution of a miniaturized silicon through-substrate split-ring resonator microplasma source [J]. ***Journal of Microelectromechanical Systems***, 2014, 23 (6): 1340-1345.

[14] Cui N D, Kou J T, Liang J Q, et al. Athermal biosensor based on three waveguide micro-ring resonators [J]. ***Chinese Optics***, 2014, 7(3): 428-434.

[15] Amiri I S, Ali J. Simulation of the single ring resonator based on the Z -transform method theory [J]. ***Quantum Matter***, 2014, 3(6): 519-522(4).